The active tectonic landscape of Lake Ohrid (FYR of Macedonia/Albania)

Nadine Hoffmann

RWTH Aachen University, Neotectonics and Natural Hazards Group, Aachen, Germany

ABSTRACT

The study area at the Lake Ohrid Basin is located on 693 m a.s.l. at the south-western border of the Former Yugoslavian Republic of Macedonia with Albania. It is a suitable location for neotectonic studies. It exhibits a large variety of morphological expressions associated with the seismic activity of the region. Linear bedrock fault scarps give the relief on both sides of the lake a staircase-like appearance; other features are wine-glass shaped valleys and triangular facets. These often short living features are used to identify active faults and to parameterise palaeoearthquakes (slip rates, subsidence and erosion). According to the results of fault scarp profiling a halfgraben shape of the basin is proposed with the west coast being dominated by mass wasting processes most likely triggered by seismic events.

1. Introduction

Lake Ohrid considered as an ancient lake was tectonically formed during the late Tertiary in the extensional periods of the Paleogene and Neogene [Dumurdzanov et al. 2004]. The region along the southernmost border of the Former Yugoslavian Republic of Macedonia (from hereon referred to as Macedonia) with Albania evolved as an extensional basin-and-range-like system within the Albanides, which is influenced by the roll-back and detachment of the subducted slab of the Northern Hellenic Trench [Hoffmann et al. 2010]. The Lake Ohrid Basin itself, located on 693 m a.s.l., is limited by major N-S trending active faults. These affect the appearance of the surrounding mountain ranges of Galicica and Mokra with heights of max. 2,265 m (Figure 1).

The geology of the basin is dominated by two major units: The Mirdita Ophiolite Zone (internal zone of the Albanides) and the Korabi Zone (Western Macedonian Zone) (for details see Hoffmann et al. [2010] and Figure 1). The units of the Korabi Zone are thrust over the Mirdita Zone ophiolites. This results in a division of the basin in two parts, where the west, southwest and south is dominated by Triassic conglomerates and Jurassic ophiolites and the eastern flank, north and northwest is dominated by Paleozoic metamorphic rocks, Triassic limestones and Quaternary sediments. This geological and geodynamic setting results in a diverse seismic landscape [Michetti and Hancock 1997, Michetti et al. 2005] that provides tectonically induced landscape features, which are still preserved in the surroundings of Lake Ohrid (see Figure 2). The range bounding faults at the eastern and western shore trend NW-SE and NE-SW but follow in general the N-S trend of the youngest deformation phase (see Hoffmann [2013] for details). They are therefore activated or reactivated by the E-W trending extensional regime dominating the basin since Holocene. This study proves the link between landscape evolution and tectonic activity in the region.

2. Seismicity

The Ohrid-Korca zone is regarded as one of the zones with the highest seismic hazard in Albania/Macedonia with frequent moderate earthquakes in the last few centuries [Muco 1998, Goldsworthy et al. 2002, Aliaj et al. 2004, NEIC 2013]. As evidenced by fault plane solutions of earthquakes the main structural sections of the eastern Adriatic coast can be subdivided into a compressional coastal domain, followed by a narrow zone of transition west of Lake Ohrid; the extensional domain is located further east in which the Neogene basins formed [Hoffmann et al. 2010, Reicherter et al. 2011, Hoffmann 2013]. Earthquake focal mechanisms show active N-S normal faulting with horst and graben structures in a basin and range like environment.

Several earthquakes have already been documented in historical times. The cities of Ohrid and Skopje (110 km NNE of Ohrid) have been destroyed by the A.D. 518 earthquake so that almost the entire city of Ohrid had to be rebuilt [Petrovski 2004]. The description of Ambraseys [2009] suggests an event of a

Figure 1. Overview and lithological map of Lake Ohrid including locations of figures. Compiled after Dumurdzanov and Ivanovski [1977], Premti and Dobi [1994].

minimum intensity of X or XI and a magnitude of 7 or more (according to Wells and Coppersmith [1994]). Other significant events occurred in February A.D. 548; April 3, 1673, February 7, 1871, September 10, 1889, and September 28, 1896, which was M 6.7 according to Papazachos and Papazachou [1997]; [Ambraseys and Jackson 1990, Goldsworthy et al. 2002, Ambraseys 2009].

The strongest event ever measured since the beginning of instrumental seismicity records in the early 20th Century was the February 18, 1911, earthquake at 9.35 p.m. It occurred in the Ohrid-Korca area (40.9°N, 20.8°E) at a depth of 15 km and a magnitude 6.7 (corresponding to EMS X) [Milutinovic et al. 1995, Muco 1998].

More recent events are the September 6, 2009, Mw 5.6 event in Debar, Albania (41.46° N, 20.41° E; focal depth 2 km, normal faulting) and the June 8, 2012, Mb 4.4 earthquake 15 km northeast of Ohrid city (41.24° N, 20.90° E; focal depth 10 km, normal faulting; EMSC

[2013], NEIC [2013]). Events with magnitudes below Mw 5 occur more frequently (e.g. February 8, 2012, Mw 4.0, 40.81° N 20.53° E; November 26, 2012, ML 2.9, 40.88° N 21.11° E; EMSC [2013]).

GPS velocity models from Burchfiel et al. [2006] and Caporali et al. [2009] show a uniform SSE migration of Macedonia together with western Bulgaria as a joint crustal piece with 3-4 mm/a. Burchfiel et al. [2006] estimate present day slip-rates of max. 2 mm/a on "NNW-striking normal faults and associated strike-slip faults with right-lateral displacement" but with a very high uncertainty due to a coarse-meshed GPS network [see also Hoffmann 2013].

3. Methods

Preservation of several meter high coseismic fault scarps is a function of reduced production and mobility of sediments along the slope, persistent climatic conditions, and cumulative earthquake events along the same fault (tectonic slip rate > erosion rate). During glacial conditions enhanced sediment mobility was faster than fault slip movement; no or only minor scarps developed [Papanikolaou et al. 2005]. This is broadly confirmed by cosmogenic dating of fault scarps in Greece (Sparta Fault, Peloponnesus [Benedetti et al. 2002]; Kaparelli Fault, Greece [Benedetti et al. 2002]) and Italy (Magnola Fault, Apennines [Palumbo et al. 2004]). The well preserved hard rock fault scarps in the Lake Ohrid Basin, especially those made up of limestones and displaced against Quaternary sediments, are also considered to be post-glacial (or Late Pleistocene).

More than 30 profiles of fault scarps were generated from scarps found in limestones and harzburgites and a few found in sandstone and serpentinite following the method of Papanikolaou et al. [2005]. Most of the morphologic scarps could be identified as fault scarps by kinematic indicators, mainly slickensides, on the fault planes. Field measurements were carried out by laying 1 m wooden poles on the slope surface perpendicular to the strike of the fault plane. The wooden poles were arranged along a tape measure which was adjusted to have the same dip direction. The inclination of the profile was then measured on each wooden pole at 1 m intervals with a compass clinometer. In order to reconstruct the offset, a minimum of 40 m length was considered. Only natural scarps that have not been anthropogenically influenced were measured. Most outcrops are therefore located in remote areas and hard to access. Obviously modified locations e.g. by military trenches or road construction were not taken into consideration for the final analysis. Also scarps, that are subject to unusually high erosion or sedimentation rates (e.g. sandstone or serpentinite scarps) were not investigated.
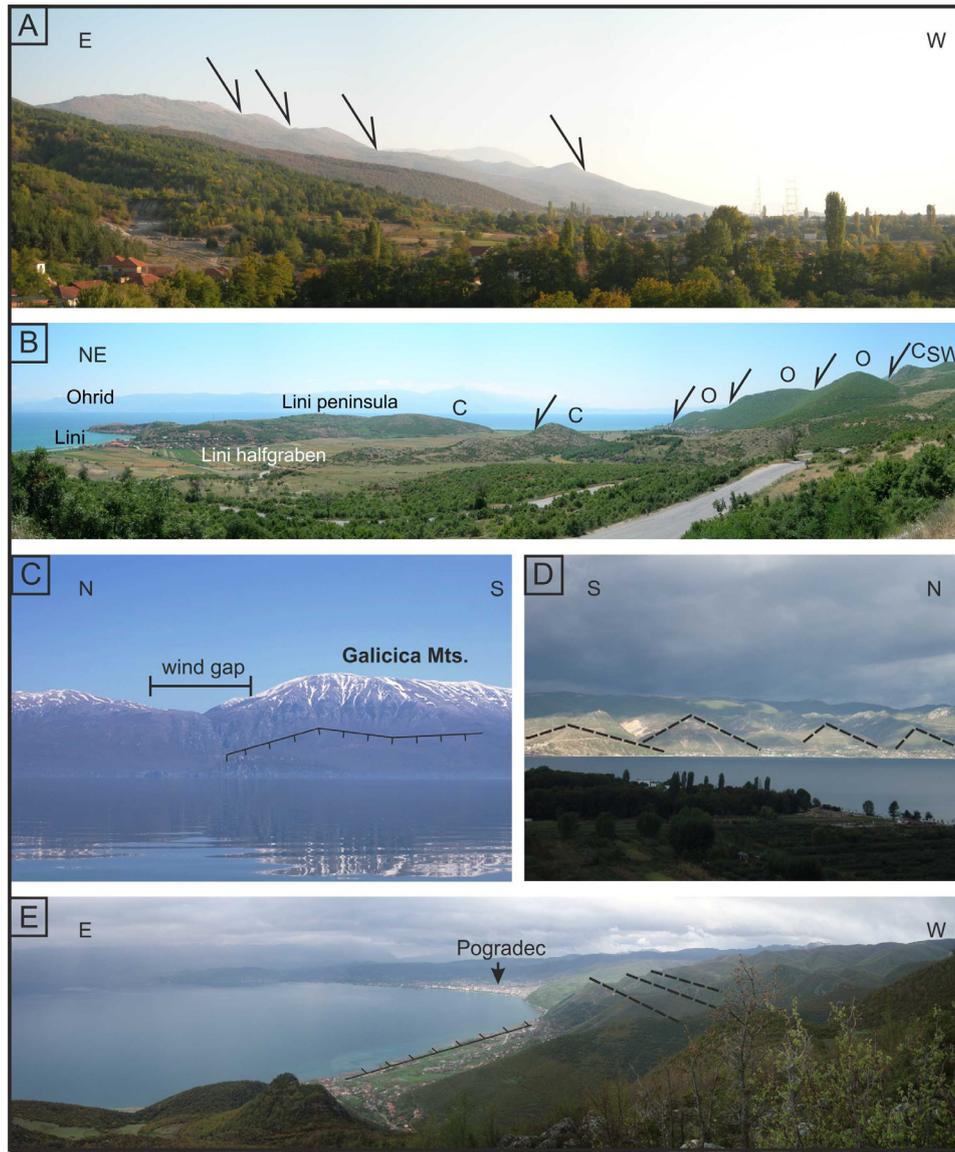
Figure 2. (A): Staircased landscape at the slope of Galicica Mountains. Arrows show orientation of normal faults. View to south. (B): Panoramic view of Lini Peninsula and Mokra Mountains showing tectonic features. o= ophiolites, c=carbonates, arrows indicate orientation of normal faults. View to southeast. (C): E-W trending wind gap at Galicica Mountains, probably developed as an old fault or discharge connection between Lake Prespa and Ohrid. Black line shows fault trace. View to east. (D): Triangular facets on the west coast (Hudenisht area). View to west. (E): Panoramic view of the southwestern coast. Dashed line shows inferred fault traces (see also Figure 1). Note the fault-cut alluvial fan. View to south.

In general a scarp can be divided into a number of sections: upper slope, degraded scarp, free face, colluvium and lower slope. These sections were defined in each profile and the mean dip of the upper and lower slopes was determined. To construct the thickness of the colluvium and the theoretical edge of the scarp before erosion, the slopes were geometrically extended towards the free face. From this it was possible to calculate the theoretical offset along the rupture. The thickness of the colluvium was observed and estimated in the field. Using the data from these profiles, a complete geometry of diverse fault scarps measured all over the basin can be obtained.

To quantify the stages of dissection along triangular facets found in the southwest and northeast of the basin, mountain front sinuosity indices were calculated by using the method proposed by Bull [2007]; Bull and McFadden [1977]. The sinuosity of the mountainfront is defined by the ratio of the length of the mountain-piedmont junction Lj to the straight length of the mountainfront Ls.

$$J = Lj/Ls$$

Other geomorphic indices such as valley floor width-to-height ratio, or longitudinal river profiles were not taken into account as the different lithologies in combination with their different resistivities to weathering produce such high uncertainties, that the definition of activity classes throughout the basin did not produce reliable results.
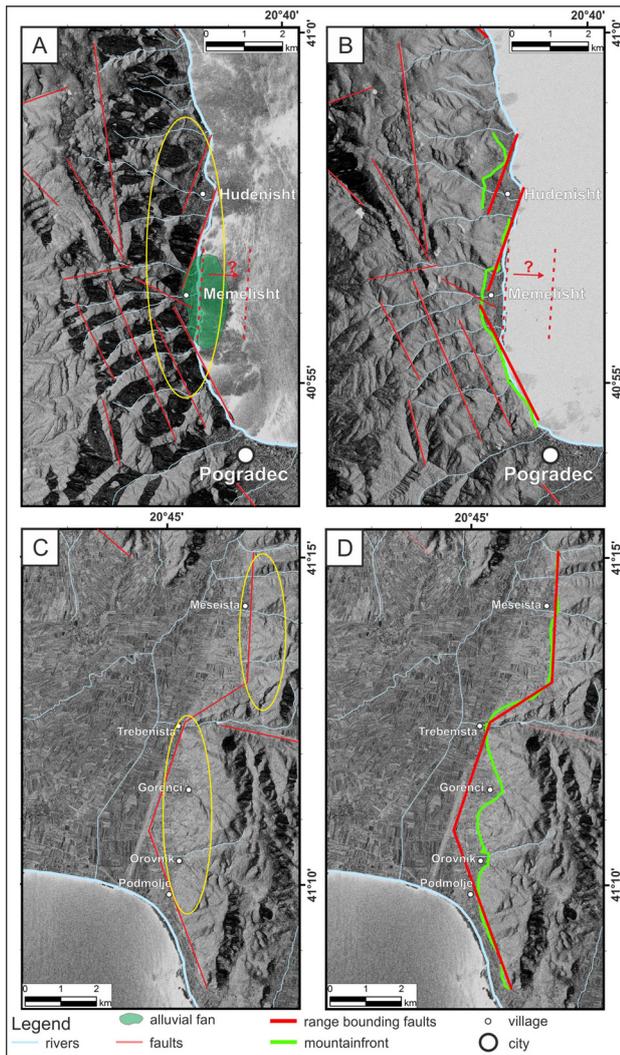
Figure 3. Mountainfront Sinuosity Index for two sites at Lake Ohrid, both exposing triangular facets in various states of degradation. (A): Map view showing main faults in the Hudenisht area. Yellow ellipse shows location of triangular facets and associated alluvial fans. (B): Mountainfront and range bounding faults in the Hudenisht area. (C): Map view showing main faults in the Meseista and Gorenci area. Yellow ellipse shows location of triangular facets and associated alluvial fans. (D): Mountainfront and range bounding faults in the Meseista and Gorenci area.

4. Triangular facets

Along both the eastern and the western coastlines abundant triangular facets with hanging valleys or wine-glass shaped valleys, which dissect the faceted spur ridges, are found. Triangular facets are the result of base level fall along a mountain ridge either by lake (or sea-) level fall, the melting of glaciers or by normal faulting events. The triangular facets at Lake Ohrid partly exhibit slickensides on their fault planes pointing to normal faulting (for details on palaostress data see Hoffmann [2013]) and are therefore considered to be of tectonic origin. With successive faulting events a new free face is created and the valleys are interrupted and thus becoming hanging valleys. The base level fall and incision of streams divides the hillslope into several

drainage basins resulting in the triangular shape of the mountainfront. Typical for active triangular facets systems is a straight mountain piedmont junction and narrow valleys.

The observed triangular facets, which are related to active faults, are important landforms along the N-S running borders of Lake Ohrid and can be found at two locations (see Figure 3). One is in the southwest above Hudenisht (Figures 3A,B and 2D), the second is in the north close to the villages of Trebenista and Gorenci (Figure 3C,D).

In times of quiescence the mountain fronts are building up sinuosity with the retreat of the range bounding fault and the valleys become wider. The initial streams develop and become small elongated watersheds. The expression of triangular facets is highly connected to the erosional resistance of rocks and the climatic conditions as shown by Bull [2007].

Along the western shore of Lake Ohrid, repeated triangular facets (Figure 2D) originate in stepped normal faults. The heights of the facets range between 162 m and 210 m and have a length at the mountainfront piedmont junction between 570 m and 750 m. The river courses are partly deflected testifying to parallel normal fault activity with a certain oblique component, e.g. near Hudenisht (Figures 3A and 2E), where four normal faults form a landscape with a stepped escarpment. The mountainfront sinuosity indices calculated for the Hudenisht area provide evidence for the relatively young age of the triangular facets; the material along the south western coast is relatively easier to erode. For the southern part of the Hudenisht area a mountainfront sinuosity index of 1.091 was calculated and a stage of dissection between 2 and 3 was determined [after Bull 2007]. For the northern part of the Hudenisht area, a mountainfront sinuosity index of 1.075 and a stage of dissection 5 was calculated [after Bull 2007]. Furthermore, in front of the mountain range in the southwestern part of Lake Ohrid, inactive alluvial fans form a linear coastline instead of a lobe shaped fan complex (Figure 2E). The shape of the alluvial fans with the linear cut edge could be interpreted as drowned fans by Holocene lake level rise. However, high resolution hydroacoustic surveys demonstrated shoreline parallel active faults offshore [Lindhorst et al. 2010] which is more likely the reason for the cut off fans.

Triangular facets in the north of Lake Ohrid are more heavily eroded and exhibit large alluvial fans in between the faceted spurs. The heights of the facets here range between 162 m and 250 m and have a length at the mountainfront piedmont junction between 750 m and 1200 m. A mountainfront sinuosity index of 1.13 was calculated here, although the area seems to be a lot

location	coordinates	height [m a.s.l.]	lithology	throw free face [m]	heave free face [m]	offset free face [m]	throw construction [m]	heave construction [m]	offset construction [m]	fault angle [°]	rotation [°]	slope angle upper [°]	slope angle lower [°]	corrected fault angle [°]
Bebien	41°12'35.1"N 20°37'54.5"E	817	limestone	21.96	8.87	23.68	21.96	8.87	28.13	21.7	2.5 ccw	2.5 ccw	23.27	46.24
Boces upper part	41°02'50.7"N 20°37'31.1"E	965	limestone	11.94	24.86	27.58	19.36	30.99	36.54	39.5	17.5 ccw	17.5 ccw	2.5 ccw	79
Boces lower part	41°02'50.7"N 20°37'31.1"E	965	limestone	23.05	20.10	30.58	25,87	19.94	32.66	55	2.5 ccw	2.5 ccw	30.8	79.5
Boces softrock	41°02' 35"N 20°37'17.9"E	956	ophiolith	2.65	9.51	9.87	2.65	9.51	9.87	16.2	4.4 ccw	4.4 ccw	30.8	42.6
Delogozdi 1	41°15'29.3"N 20°43'56.2"E	898	limestone	5.54	1.23	5.67	7.21	0.99	7.28	83	x	21	21	x
Delogozdi 2	41°15'25.6"N 20°43'53.5"E	882	limestone	6.11	3.61	7.09	18.34	10.08	20.93	61	x	9	25	x
Dzepin	41°15'18.1"N 20°44'08.1"E	943	limestone	12.09	14.07	18.55	20.29	14.28	24.81	55	x	21	21	x
Elen Kamen	41°08'23.6"N 20°38'51.4"E	767	limestone	25.44	8.28	26.75	32.21	6.35	32.83	78.9	x	21.9	2.3	x
Elsani 1	41°01'21.3"N 20°49'19.5"E	1076	limestone	10.57	3.89	11.26	15.00	4.13	15.56	75	x	5.6	5.6	x
Elsani 2 upper part	41°01'19.6"N 20°49'18.0"E	1040	limestone	3.01	0.63	3.07	3.06	0.20	3.06	75.8	x	19.6	19.6	x
Elsani 2 lower part	41°01'19.6"N 20°49'18.0"E	1038	limestone	4.83	2.75	5.55	5.39	3.03	6.18	61.4	x	19.6	19.6	x
Elsani 3	41°01'15.1"N 20°49'21.0"E	1092	limestone	3.55	4.14	5.45	5.98	3.3	6.83	61.2	4.5 ccw	11.3	29.7	87.7
Elsani 4 total	41°01'11.2"N 20°49'26.1"E	1125	limestone	23.81	19.83	30.99	41.35	12.06	43.07	70.5	x	21.6	32	x
Elsani 5	41°02'3.9"N 20°48'43.3"E	856	limestone	120.86	127.33	175.55	120.86	127.33	175.55	42.5	x	16.44	?	x
Hudenisht	40°57'08.9"N 20°37'42.8"E	1121	limestone	24.69	14.21	28.48	58.47	9.35	59.21	81	5 ccw	5 ccw	25	108
Hudenisht softrock	40°57'12.6"N 20°38'28.3"E	761	sandstone	26.88	47.13	54.25	29.24	4.68	29.61	29.9	x	10.5	2.9	x
Koritsi Rid	40°57'55.9"N 20°48'40.8"E	1425	limestone	18.78	13.06	22.87	29.56	15.66	33.45	62	11 cw	11 cw	38	95

Table 1 (continued on next page).

location	coordinates	height [m a.s.l.]	lithology	throw free face [m]	heave free face [m]	offset free face [m]	throw construction [m]	heave construction [m]	offset construction [m]	fault angle [°]	rotation [°]	slope angle upper [°]	slope angle lower [°]	corrected fault angle [°]
Lako Signoj upper part	40°58'11"N 20°48'7.1"E	1084	limestone	11.04	2.38	11.29	14.48	1.44	14.55	85.5	x	25.5	25.5	x
Lako Signoj lower part	40°58'11"N 20°48'6.1"E	1076	limestone	10.66	9.55	14.31	12.51	9.02	15.42	54	x	25.5	25.5	x
Lini 1	41°04'10.4"N 20°37'31.6"E	908	limestone	6.96	5.72	9.01	9.40	2.9	9.83	81.7	x	20.4	20.4	x
Lini 2	41°04'11.0"N 20°37'31.1"E	897	limestone	17.57	45.63	48.89	17.57	45.63	48.89	21.2	x	19.94	19.94	x
Lini 3	41°03'57.7"N 20°37'57.4"E	759	limestone	8.61	9.66	12.93	6.40	2.45	6.85	69	x	21.47	29	x
Memelisht	40°55'10.1"N 20°38'14.9"E	947	limestone	31.78	30.34	43.93	27.69	13.35	30.74	64	x	17.5	22	x
Memelisht softrock	40°56'31.30"N 20°37'27.60"E	1040	harzburgit	13.06	51.86	53.48	13.06	51.86	53.48	15.4	4.3 ccw	4.3 ccw	26.9	x
Pestani 1	41°00'44.7"N 20°48'47.3"E	822	limestone	2.84	0.89	2.97	4.93	1.16	5.06	77	x	8	8	x
Pestani 2	41°00'47.4"N 20°48'48.2"E	799	limestone	5.22	3.15	6.09	5.48	1.92	5.80	71	1.5 cw	1.5 cw	28	94.5
Piskupat	41°02'16.2"N 20°37'33.9"E	916	ophiolite/limestone	25.40	34.00	42.44	31.82	40.33	51.37	39	22 ccw	22 ccw	11	83
Sveti Arhangel 1	41°06'27.4"N 20°37'56.5"E	840	limestone	42.98	0.75	42.98	46.86	0.84	46.87	89	x	27.2	27.2	x
Sveti Arhangel 2	41°06'28.5"N 20°37'55.4"E	845	limestone	50.37	7.97	51.00	57.83	9.09	58.54	81	x	28.12	28.1	x
Sveti Stefan	41°04'22.5"N 20°48'19.1"E	1031	limestone	7.38	3.69	8.25	10.2	0.86	10.24	85	x	2.5	27	x
Sveti Spas	40°59'30.1"N 20°48'43.8"E	1070	limestone	3.84	1.00	3.96	4.38	0.97	4.48	77.3	1.5 cw	1.52	23.25	100.8
Velestovo 1	41°5'14.5"N 20°49'17.2"E	985	limestone	11.45	11.02	15.89	12.5	11.14	16.74	65	x	0.98	24.3	x
Velestovo 2	41°5'6.3"N 20°49'23"E	1004	limestone	41.95	39.35	57.51	47.83	36.21	59.99	87.3	x	6.23	28.88	x
Velestovo 3	41°04'16.5"N 20°49'08.0"E	1250	limestone	29.17	21.78	36.40	34.22	25.74	42.82	53	11.5 cw	11.5 cw	26.8	86.5

Table 1 (continued from previous page). Table of all scarp profiles, including position, lithologies and geometric parameters.

less active than the Hudenisht area and a stage of dissection between 3 and 4 was determined [after Bull 2007]. Values of the mountainfront sinuosity index between 1.0 and 1.5 reflect a highly active mountainfront after Bull [2007].

5. Scarp profiles

Bedrock fault scarps are the most visible land forming features that are observed in the Ohrid region. They account for a high percentage of the morphological expressions within the basin. According to the hypothesis of Benedetti et al. [2002] and Papanikolaou et al. [2005], they are considered to be post-glacial, as the slip-rate along the fault planes needs to be higher than the erosion rate to preserve the step-like morphology. Bedrock fault scarps are found in all lithologies around Lake Ohrid and are well preserved in limestones and ophiolites. 31 fault scarps were measured throughout the basin: 14 along the western graben shoulder, 14

along the eastern graben shoulder and 3 in the north of the basin (see Table 1). Here, a few examples are presented in detail.

5.1. Lako Signoj

The Lako Signoj limestone scarp is composed of two single steps (for location see Figure 1). The upper scarp shows an offset of about 11 m, the lower one of about 14 m (Figure 4). The most visible difference between the two is that the horizontal displacement significantly varies (2.3 m upper scarp and 9.5 m lower scarp) while the vertical displacement is relatively uniform at around 11 m. The dip angle of the upper fault is 85.5°; it is quite normal for these limestone faults to be very steep and show angles close to vertical. In contrast, the dip angle of the lower fault is only 54°. The upper slope is heavily degraded close to the edge of the fault. Therefore, the upper edge of the fault cannot clearly be defined; there might have been a detached
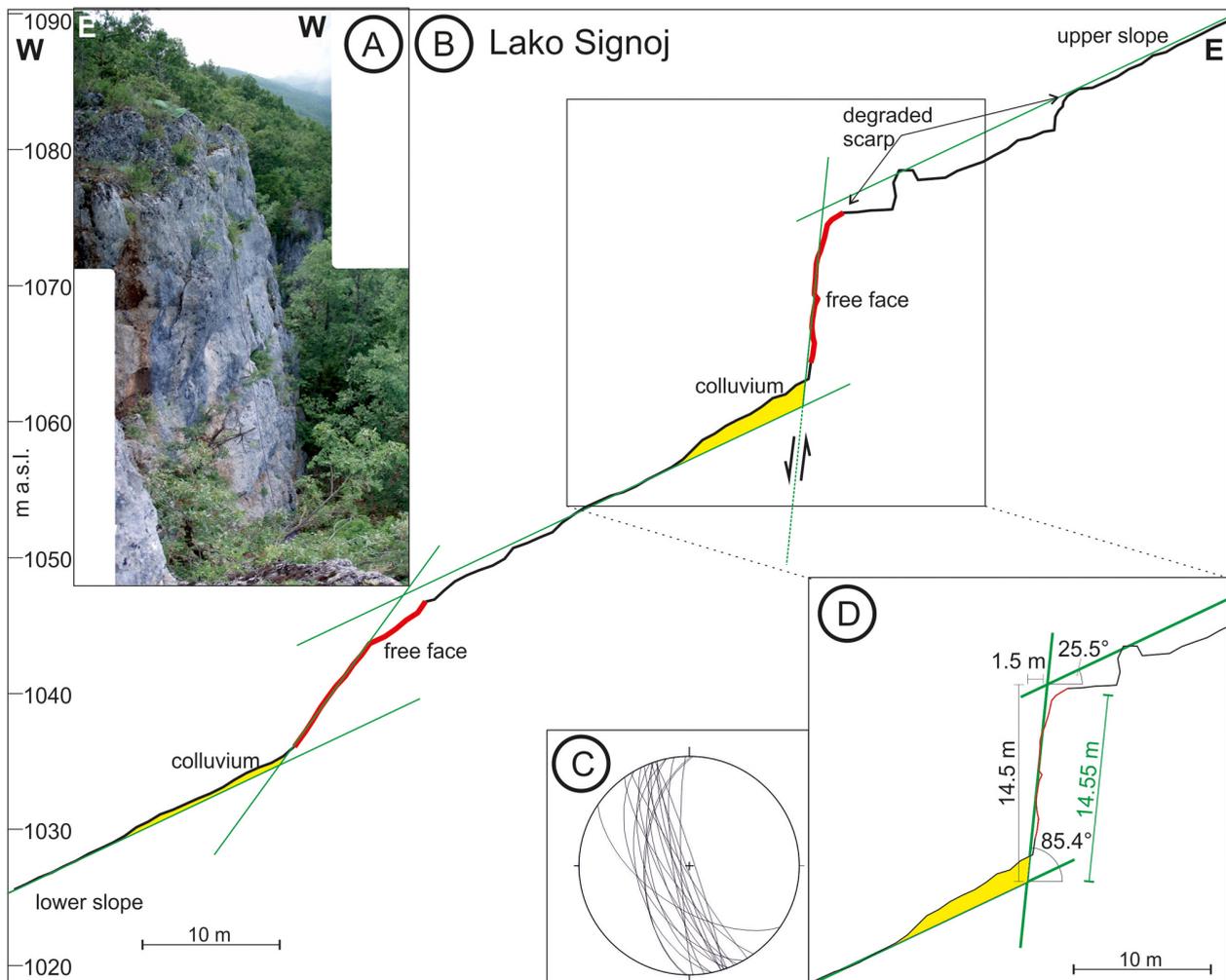
Figure 4. (A): Photograph of the Lako Signoj scarp. Yellow line gives the approximate position of the profile. (B): Complete profile and geometric reconstruction of the Lako Signoj fault (40°5811111N, 20°4810711E; 1076 m a.s.l. for location see Figure 1). Only the upper scarp was analysed in detail. No vertical exaggeration. Green lines show constructed angles of upper and lower slope and the fault plane. Red lines indicate the free face measured in the field. The colluvium (marked in yellow) is constructed from field data. (C): Stereonet plot of measurements from the fault plane. (D): Dip angles and offset derived from geometric construction.
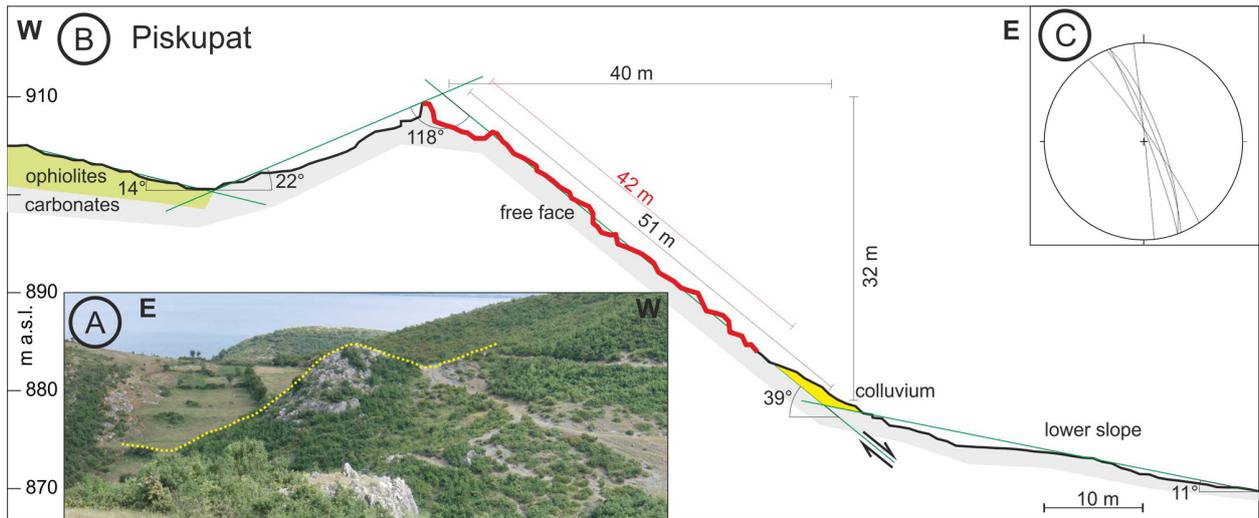
Figure 5. (A): Photograph of the Piskupat scarp. Yellow line gives the approximate position of the profile. (B): Complete profile and geometric reconstruction of the Piskupat fault (41°0211511N, 20°3713211E; 905 m a.s.l. for location see Figure 1). No vertical exaggeration. Green lines show constructed angles of upper and lower slope and the fault plane. Red lines indicate the free face measured in the field. The colluvium (marked in yellow) is constructed from field data. (C): Stereonet plot of measurements from the fault plane.

block at the top giving it its distinct shape. The volume of colluvium between both scarps is very small compared to the volume of the upper slope's missing material. The 25.5° slope gradient is measured for all three slopes. The lower scarp seems to be less eroded and exhibits even smaller volumes of colluvium. The ground cover directly below the lower scarp is composed of some tens of centimetres of soil. Along the relatively steep slopes the eroded material has been quickly transported further downslope especially with the beginning of snowmelt in spring. The reconstructed slip of both scarps is about 15 m each.

Figure 6. Concept of fault scarp evolution at the Piskupat fault. o=ophiolite, c=carbonate. Planar rotational faults evolve under an extensional stress regime. Later these are subject to erosion. As the erosion strips off the ophiolites from the underlying carbonates the shape of the fault can evolve. The halfgraben below the fault is filled with debris from the surrounding.

5.2. Piskupat

The Piskupat fault scarp is somewhat more unique than the other faults found in the Lake Ohrid Basin (for location see Figure 1); there are quite a few similar to this one on the west coast, but they were not accessible. The fault plane angle is 39° with well distributed colluvium below (Figure 5). The lower slope has a gradient of 11° to the east. The upper slope, which is made up of ophiolites, has a gradient of 14° towards east. This is slightly more than the lower slope. The key feature is the change of lithology which causes the specific morphological shape. The upper slope is made up of ophiolites while the scarp itself and the lower slope are made up of limestones. The ophiolites have been eroded more quickly due to the different resistance to weathering. As a consequence the limestones are now exposed and preserved as a morphological scarp (see Figure 6). The eroded material, that should be found in the halfgraben, was most probably transported to the north and into the lake via a small river valley.

The contact between ophiolites and limestones mimics the presence of a fault plane, if looking at the morphology of the scarp, only. But the actual fault plane is not located in the small halfgraben where the change of lithology was observed; it must be located further up to the west. This assumption considers erosional effects that cause the contact point of lithologies to migrate upslope (see Figure 6).

6. Sorting out age issues at Dolno Konjsko

At the village of Dolno Konjsko (Figure 1) a palaeosol is preserved in the hanging wall of an active normal fault (Figure 7A), where Quaternary sediments are displaced against Jurassic limestones. The palaeosol

was dragged into the fault with fault movement and is, therefore, a marker for the activity in the basin. OSL dating was performed at this location to get a minimum age of the last movement along this fault. The probing locations are marked in Figure 7B. Only the sample of the stratigraphically youngest sediment delivered reproducible results, as the OSL signal was already in saturation for samples OH2, OH3 and OH4 and therefore did not give an age determination.

The OH1 sample delivered a Pleistocene age dated to 11 ± 1.7 ka. This period can be assigned to the Younger Dryas stadial, which marks the transition between Pleistocene and Holocene. The material deposited here is composed of unrounded large limestone clasts originating from the Triassic limestones of the Galicica mountains. Erosion and transportation mechanisms are favoured by the scarce vegetation and dry soils [Vogel et al. 2010]. Below, the palaeosol is characterised by red coloured soil with root remnants and much smaller grain sizes than the clasts above and below. This portion is ascribed to the Alleröd, which represents the last interstadial with warmer climate conditions allowing soil formation. Vogel et al. [2010] also found evidence for cold winters and higher spring-summer temperatures corresponding to this age in offshore sediment cores. Below again a section containing large limestone clasts occurs pointing to colder conditions and high erosion rates as present in the Older Dryas.

The outcrop can be therefore divided into 4 sections:

– recent soil in red colour (Holocene)

– upper part with large clasts; light brown colour (sample OH1; Younger Dryas)

– red coloured, dragged palaeosol and plant remnants, roots (sample OH2; Alleröd interstadial)

– lower part with large clasts; light brown color (sample OH3 and OH4; Older Dryas).

This outcrop shows that normal faulting processes took place already during Pleistocene times. But erosion erased any geomorphological evidence of faulting (e.g. fault scarps) so that the sense of slip and the orientation of the fault can only be estimated by the dragged palaeosol. This leads to the assumption that the fault scarps exposed around Lake Ohrid must at least be younger than the Alleröd interstadial or 11 ka, respectively.

7. Discussion

The Lake Ohrid Basin, especially the eastern (Galicica Mountain range) and western flanks (Mokra Mountain range), are dominated by normal faulting, and the northern and southern parts (the plains of Struga and Pogradec) [Hoffmann et al. 2012] are dom-
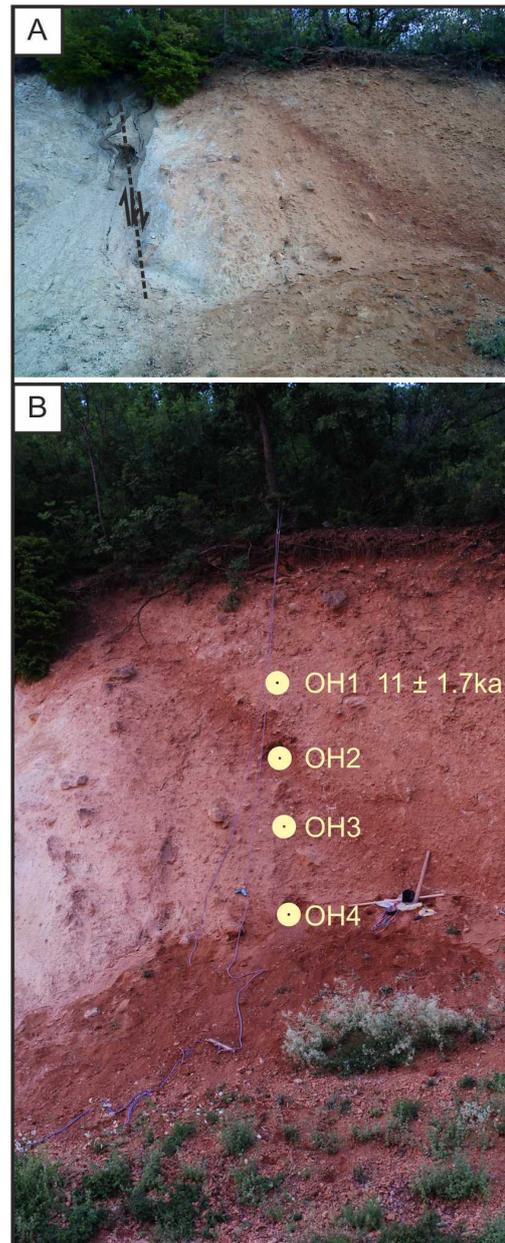
Figure 7. Fault at Dolno Konsjko Quaternary sediments are displaced against limestones. OSL sampling locations and associated ages are marked.

inated by clastic input. In general, the north and the south do not seem to be as active although indications for tectonic activity were observed here.

The geology of the basin, which is dominated by two major units, plays a major role in the distribution of the morphotectonic features [Hoffmann et al. 2010]. In the Mirdita Ophiolite Zone, Triassic conglomerates and Jurassic ophiolites show weak resistance to weathering processes and therefore exhibit less or less pronounced fault scarps. The only exceptions to this are the Upper Cretaceous limestone caps along the southwestern shoreline. In contrast, the Korabi Zone is dominated by Palaeozoic metamorphic rocks, Triassic limestones and Quaternary sediments, which are more resistant to weathering and therefore create the stair-

case-like morphology that is typical for the basin. The result of the lithological zonation is an inhomogeneous morphological surface expression within the influence of the same stress field. Besides that, it can be observed that the NW-SE striking lithological contacts are cross-cut by the N-S strike of the basin and its young normal faults. Older structural features like folds, faults, and joints are also cut by these N-S trending normal faults.

The main trend of the fault scarps is N-S, with variations of $\pm 20°$, and dips ranging between $42°$ and $85°$ (along the western shore towards the east, on the eastern shore to the west), hence, forming a graben structure. This observation correlates with the data from palaeostress analyses by Hoffmann [2013], where the E-W extensional phase is the youngest.

Of 36 measured faults, six were not analysed as the data quality was not sufficient. Three of these are located in softrock and did not qualify for the calculation of mean values and slip rates. 19 fault scarps can be defined as planar non-rotational faults [Wernicke 1981, Wernicke and Burchfiel 1982, McClay and Ellis 1987] with an upper slope angle that mostly matches the lower slope angle. These faults show mainly a vertical displacement component. This fault type is generally found at symmetrical grabens where fault bound blocks are downthrown.

Another 11 scarps show rotation towards the fault plane, only four of these are located on the east coast. Rotation takes place around an axis parallel to the strike of the fault [Twiss and Moores 2007]. The blocks can rotate until they reach a very low dip and therefore can accommodate large extension. There are three main mechanisms for the observed tilting of the fault blocks:
– Listric faulting with associated rollover anticlines, or sets of antithetic faults in the hangingwall;
– Listric faulting with the development of synthetic fault blocks that act like dominoes. Towards the basin centre, the dip of the faults becomes shallower and horizontal displacement increases, while the angle between bedding and fault planes remains constant;
– Sets of parallel listric faults with increasing dip of the bedding with distance to the main fault and therefore decreasing dip of fault planes with distance to the main fault.

The rotation of the scarps in the Ohrid Basin varies between $5°$ and $11°$ to horizontal, with some exceptions. The influence of erosion and the true rotation can only be estimated. The mean slope angle is $22°$ throughout the basin. This angle plus the tilt towards the fault have been added to all rotated faults to determine the shape of the corrected fault angles. The result is that most of the corrected angles range between the high $70°$s, or low $80°$s. Only Hudenisht, Koritsi Rid,

Pestani 2 and Sveti Spas reach angles higher than $90°$. This implies that, in most cases, a rotation of around $22°$ is sufficient to reconstruct the original shape of the faults. Therefore, the domino or planar rotational faults model [Wernicke 1981, Wernicke and Burchfiel 1982, McClay and Ellis 1987] (see Figure 6) is a possible deformation mechanism. Rollover anticlines and antithetic faults were not observed onshore, but were both found in offshore seismic data by Lindhorst et al. [in press]. In addition, fault plane dips become shallower towards the basin centre ($25°$ at the Lini Fault after Lindhorst et al. [in press]), which points to the model of parallel listric faults. The fault activity is seen in multi-channel-seismic sections with scarps and syn-tectonic rotation of strata [Lindhorst et al., in press]. But as the dip of beddings was not measured onshore, neither a definite statement can be given, nor the amount of extension can be calculated. Most likely the basin shows two modes of listric faulting and therefore exhibits a combination of rotated blocks and sets of parallel listric faults.

The mean fault scarp height for the west coast is 38.5 m (measured), 39.5 m (reconstructed); for the east coast it is 25 m (measured) 29.3 m (reconstructed); and for the north it is 10.4 m (measured), 17.6 m (reconstructed). The mean dip angle is $55°$ for the west coast, $67°$ for the east coast, and $49°$ for the north. Only on a local level it can be observed that those scarps, which are located further away from the centre of the basin, are in general the higher ones. This observation is probably related to the small-scale disposition of the basin, so that lithology, joints, the impact of the hydrological system, and to a smaller extent the human influence control the expression of the scarp profiles.

The Dolno Konjsko outcrop shows that fault scarps with a distinct morphological relief around Lake Ohrid are most likely younger than 11 ka. Because of this assumption and data from other authors [Papanikolaou et al. 2005], slip rates were calculated, stating a postglacial development of the exposed fault scarps for the last 15 ka $\pm$ 3 ka. Slip rate values range between 0.33$\pm$0.9 mm/a and 3.90$\pm$1.0 mm/a, respectively. These values exceed by far the sliprates calculated by [e.g., Benedetti et al. 2003] who were working on well constrained dated limestone fault scarps in Greece with slip rates of 1.0 mm/a at the Sparta fault. Considering the seismic activity of the Ohrid-Korca area this result is not satisfactory. The strong variability of scarp heights (some meters to some 10 meters) in the research area would mean that:
(1) the postulated age of the higher scarps is simply too young, or
(2) the higher the scarp is, the faster the movement on the fault plane must be, unless the beginning of

scarp preservation can be pinpointed to a certain time.

Comparing slip data from Papanikolaou et al. [2005] with data from the Ohrid Basin shows that slip rates increase with the amount of slip which means in return, that the simple idea of postglacial development of fault scarps is not sufficient to explain the height of fault scarps, specially taking into account that there is no correlation between scarp height and position in the basin. The thickness of the colluvium was only constructed from the graphics and evaluated by field observations but not confirmed by drilling. In addition, spatial variations in erosion rates can be a factor that has an influence on the constructed fault geometry. This can in sum not be responsible for the differences in slip rates. A theory that could cope with the problem is the concept of "stop and go" faults. Here the older outer faults would slip every time a younger fault evolves and therefore create a higher relief than the younger fault scarp. So that when the outer fault slips with every seismic event, it is therefore higher the older it is and the more successive events it was subject to. This concept of course allows for instable slopes and mass wasting such as landsliding processes.

As the there is no pattern applicable to the locations of rotated faults, the idea is that not only the faulting mechanism but also gravitational forces play a major role in scarp displacement. In the Hudenisht area in the southeast of the basin (see Figure 3A,B) a set of four parallel faults is observed. If a closer look is taken on the river courses (Figure 3A,B), it is obvious that the valleys are not straight but show a major bend towards south at the second fault from east. This arrangement can be the result of either a transtensional component or, more likely, of mass wasting processes, where the separate blocks are transported towards the basin centre. In this process again the blocks are offset against each other and rotated. Lindhorst et al. [2012] observed a major underwater slide offshore Hudenisht ("Udenisht Slide Complex" in Lindhorst et al. [2012]) covering an area of c. 27 km^2 and extending approximately 10 km into the central basin. This slide complex is linked to N-S striking normal faults and was possibly triggered by the A.D. 515, 526 or 527 earthquake [Wagner et al. 2012]. Along with other mass wasting deposits seen in seismic data, this shows that the western slope is in general unstable. In the lake sediments this might be linked to high pore pressures, which does not apply onshore. A more sufficient explanation is that the highly fractured rocks in combination with predefined and easily reactivated fault planes acting as single blocks are prone to react to seismic events or large offshore mass wasting processes.

The triangular facets found in the lake Ohrid basin are well distributed and are only in parts highly dissected. But their general form is still obvious. Hanging valleys at the slope of Galicica and Mali I Thate mountains also testify to normal faulting events or landsliding. But as the valleys are only seasonally water bearing the erosional force for an equilibrium state is low.

According to the results of fault scarp profiling a halfgraben shape of the basin is proposed, with the western flanks dipping with 55° shallower than the east coast (67°). Also the height of the fault scarps is 39.5 m and therefore higher than fault scarps along the eastern flanks with a mean height of 29.3 m. Therefore, the western flank of the basin accommodates most of the extension. This is supported by data of Lindhorst et al. [in press] that depicted large sediment cover on the western slopes but also found evidence for active faulting especially along the Lini Fault that exhibits a shallow angle at 25°, while east is highly segmented with tilted blocks of basement. By palaoestresss analysis [Hoffmann 2013] the opening of the basin as an extensional duplex, with several parallel en-echelon faults taking up the stress was shown. To a large extent a normal component is involved in the basin formation. A master fault in the center of the basin is proposed, but it could not be clarified whether depicted sets of faults in the basin [Lindhorst et al., in press] are really the oldest or if there is another fault trace hidden beyond sediment cover. The closely spaced faults are therefore connected to the offshore faults proposed by Lindhorst et al. [in press]. The west coast is dominated by mass wasting processes most likely triggered by seismic events or by the removal of material below so that the slope becomes instable.

References

Aliaj, S., J. Adams, S. Halchuk, E. Sulstarova, V. Peci and B. Muco (2004). Probabilistic Seismic Hazard Maps for Albania, In: 13th World Conference on Earthquake Engineering (Vancouver, B.C., Canada), Paper no. 2469.

Ambraseys, N., and J. Jackson (1990). Seismicity and associated strain of Central Greece between 1890 and 1988, Geophysical Journal International, 101, 663-709.

Ambraseys, N. (2009). Earthquakes in the Mediterranean and Middle East: a multidisciplinary study of seismicity up to 1900, Cambridge University

Press, New York.

Benedetti, L., R. Finkel, D. Papanastassiou, G. King, R. Armijo, F. Ryerson, D. Farber and F. Flerit, (2002). Postglacial slip history of the Sparta Fault (Greece) determined by 36Cl cosmogenic dating: evidence for non-periodic earthquakes, Geophysical Research Letters, 29, 87/1-87/4.

Benedetti, L., R. Finkel, G. King, R. Armijo, D. Papanastassiou, F. Ryerson, F. Flerit, D. Farber and G. Stavrakakis (2003). Motion on the Kaparelli fault (Greece) prior to the 1981 earthquake sequence determined from 36Cl cosmogenic dating, Terra Nova, 15, 118-124.

Bull, W., and L. McFadden (1977). Tectonic geomorphology north and south of the Garlock Fault, California, In: D. Doehring (ed.), Geomorphology in arid regions, State University of New York at Binghamton, 115-138.

Bull, W. (2007). Tectonic Geomorphology of Mountains. A New Approach to Paleoseismology, Blackwell Publishing, 316 pp.

Burchfiel, B.C., R.W. King, A. Todosov, V. Kotzev, N. Dumurdzanov, T. Serafimovski and B. Nurce (2006). GPS results for Macedonia and its importance for the tectonics of the Southern Balkan extensional regime, Tectonophysics, 413, 239-248.

Caporali, A., C. Aichhorn, M. Barlik, M. Becker, I. Fejes, L. Gerhatova, D. Ghitau, G. Grenerczy, U. Hefty, S. Krauss, D. Medak, G. Milev, M. Mojzes, M. Mulic, A. Nardo, P. Pesec, T. Rus, J. Simek, L. Sledzinski, M. Solaric, G. Stangl, B. Stopar, F. Vespe and G. Virag (2009). Surface kinematics in the Alpine-Carpathian-Dinaric and Balkan region inferred from a new multi-network GPS combination solution, Tectonophysics, 474, 295-321.

Dumurdzanov, N., and T. Ivanovski (1977). Geological Map of the Socialist Federal Republic of Yugoslavia, Sheet Ohrid, Geological Survey Belgrad.

Dumurdzanov, N., T. Serafimovski and B.C. Burchfiel (2004). Evolution of the Neogene- Pleistocene Basins of Macedonia, Geological Society of America Digital Map and Chart Series 1, 1-20.

EMSC (2013). Earthquake database, Tech. rep., European-Mediterranean Seismological Centre; www.emsc-csem.org, http://www.emsc-csem. org (last access: 2013-09-11).

Goldsworthy, M., J. Jackson and J. Haines (2002). The continuity of active fault systems in Greece, Geophysical Journal International, 148, 596-618.

Hoffmann, N., K. Reicherter, T. Fernandez-Steeger and C. Grützner (2010). Evolution of ancient Lake Ohrid: a tectonic perspective, Biogeosciences, 7, 3377-3386.

Hoffmann, N., K. Reicherter, C. Grützner, J. Hürtgen,

A. Rudersdorf, F. Viehberg and M. Wessels (2012). Quaternary coastline evolution of Lake Ohrid (Macedonia/Albania), Central European Journal of Geosciences, 4 (1), 94-110.

Hoffmann, N. (2013). Tectonic Evolution of the Lake Ohrid Basin, Ph.D. Thesis, RWTH Aachen University.

Lindhorst, K., H. Vogel, S. Krastel, B. Wagner, A. Hilgers, A. Zander, T. Schwenk, M. Wessels and G. Daut (2010). Stratigraphic analysis of Lake-level Fluctuations in Lake Ohrid: An integration of high resolution hydro-acoustic data and sediment cores, Biogeosciences, 7, 3531-3548.

Lindhorst, K., M. Gruen, S. Krastel and T. Schwenk (2012). Hydroacoustic Analysis of Mass Wasting Deposits in Lake Ohrid (FYR Macedonia/Albania), vol. Submarine Mass Movements and Their Consequences, 245 of Advances in Natural and Technological Hazards Research, Springer Science+Business Media.

Lindhorst, K., S. Krastel, K. Reicherter, M. Stipp, B. Wagner and T. Schwenk (in press). Sedimentary and tectonic evolution of Lake Ohrid (Macedonia/Albania), Basin Research.

McClay, K., and P. Ellis (1987). Geometries of extensional fault systems developed in model experiments, Geology, 15, 341-344.

Michetti, A.M., and P.L. Hancock (1997). Paleoseismology: Understanding past earthquakes using Quaternary geology, Journal of Geodynamics, 24 (1-4), 3-10.

Michetti, A.M., F.A. Audemard and S. Marco (2005). Future trends in Paleoseismology: Integrated study of the seismic landscape as a vital tool in seismic hazard analyses, Tectonophysics, 408, 3-21.

Milutinovic, Z.V., G. Trendafiloski and T. Olumceva (1995). Disaster preparedness planning for small and medium size hospitals based on structural, non-structural and functional vulnerability assessment, World Health Organisation, Institute of Earthquake Engineering and Engineering Seismology, Skopje.

Muco, B. (1998). Catalogue of ML ≤ 3.0 earthquakes in Albania from 1976 to 1995 and distribution of seismic energy released, Tectonophysics, 292, 311-319; doi:10.1016/S0040-1951(98)00071-7.

NEIC (2013). USGS Earthquake Hazard Programme, National Earthquake Information Center, Tech. rep.; http://earthquake.usgs.gov/regional/neic/ (last access: 2013-10-21).

Palumbo, L., L. Benedetti, D. Bourles, A. Cinque and R. Finkel (2004). Slip history of the Magnola Fault (Apennines, Central Italy) from 36Cl surface exposure dating: evidence for strong earthquakes over

the Holocene, Earth and Planetary Science Letters, 225, 163-176.

Papanikolaou, I., G. Roberts and A. Michetti (2005). Fault scarps and deformation rates in Lazio-Abruzzo, Central Italy: comparison between geological fault slip-rate and GPS data, Tectonophysics, 408, 147-176.

Papazachos, B., and K. Papazachou (1997). The earthquakes of Greece, Thessaloniki Editions Ziti.

Petrovski, J.T. (2004). Damaging effects of July 26, 1963 Skopje Earthquake, Tech. rep., Middle East Seismological Forum (MESF); www.meseisforum.net (last access: June 15, 2010).

Premti, I., and A. Dobi (1994). A geological map of Albania, Sheet Masivi Ultrabazik i Shebenik- Pogradecit, Inst. Stud. Proj. Gjeologjike, Tirana.

Reicherter, K., N. Hoffmann, K. Lindhorst, S. Krastel-Gudegast, T. Fernandez-Steeger and T. Wiatr (2011). Active basins and neotectonics: morphotectonics of the Lake Ohrid Basin (FYROM/Albania), Zeitschrift der Deutschen Gesellschaft für Geowissenschaften, 162 (2), 217-234.

Twiss, R., and E.M. Moores (2007). Structural Geology, W.H. Freemann and Company, New York.

Vogel, H., B. Wagner, G. Zanchetta, R. Sulpizio and P. Rosén (2010). A paleoclimate record with tephrochronological age control for the last glacial-interglacial cycle from Lake Ohrid, Albania and Macedonia, Journal of Paleolimnology, 44, 295-310; doi:10.1007/s10933-009-9404-x.

Wagner, B., A. Francke, R., Sulpizio, G. Zanchetta, K. Lindhorst, S. Krastel, H. Vogel, G. Daut, A. Grazhdani, B. Lushaj and S. Trajanovski (2012). Seismic and sedimentological evidence 1 of an early 6th century AD earthquake at Lake Ohrid (Macedonia/Albania), Clim. Past Discuss., 8, 4333-4355.

Wells, D.L., and J.K. Coppersmith (1994). New empirical relationships among magnitude, rupture length, rupture width, rupture area, and surface displacement, Bulletin of the Seismological Society of America, 84, 974-1002.

Wernicke, B. (1981). Low-angle normal faults in the Basin and Range Province: nappe tectonics in an extending orogen, Nature, 291 (5817), 645-648.

Wernicke, B., and B.C. Burchfiel (1982). Modes of extensional tectonics, Journal of Structural Geology, 4 (2), 105-115.

---

*Corresponding author: Nadine Hoffmann,
RWTH Aachen University, Neotectonics and Natural Hazards
Group, Aachen, Germany; email: n.hoffmann@nug.rwth-aachen.de.